Published in final edited form as:
Conf Proc (Midwest Symp Circuits Syst). 2009 May 24; 2009: 2425–2428. doi:10.1109/ISCAS.2009.5118290.

Grouping of Brain MR Images via Affinity Propagation

Gang Li,
School of Automation, Northwestern Polytechnical University, Xi'an, China, lignpu@gmail.com

Lei Guo, and
School of Automation, Northwestern Polytechnical University, Xi'an, China, lguo@nwpu.edu.cn

Tianming Liu
Department of Computer Science, The University of Georgiam, Athens, GA, USA, tliu@uga.edu

Abstract

The human brain anatomy is extremely variable across individuals in terms of its size, shape, and structure patterning. In this paper, a novel method is proposed for grouping brain MR images into different patterns. This method adopts the affinity propagation methodology to partition a population of brain images into different clusters. In the affinity propagation method, the tissue-segmented and anatomically-parcellated images are used to define the similarity between brain images, in contrast to intensity-based similarity measurement used in previous methods. After clustering, in each cluster (called a sub-group) a representative exemplar image is identified as the single subject atlas for the sub-group. Meanwhile, all the subject images belonging to the same sub-group are identified. This method has been applied to the publicly available OASIS neuroimaging dataset that includes 414 subject brain MRI images. Experiments show that the method is able to group brain MR images into different patterns effectively.

I. INTRODUCTION

The human brain is a highly convoluted and complex structure. Meanwhile, the human brain anatomy is extremely variable across individuals in terms of its size, shape, and structure patterning. Given a population of human brain MR images, there inherently exist multiple patterns or sub-populations. Thus, a couple of naturally arising questions are: 1) How many patterns or sub-populations exist in a given population? 2) Which subject images belong to the same pattern? 3) Which subject image is the representative image for each sub-population? 4) Given a new subject image, which sub-population it belongs to. Meanwhile, because of the multiple patterns in a population, a single atlas is unable to appropriately represent the whole population [1], even though single atlas based methods still play a vital role in current brain image analysis [2]. Clustering brain MR images into several sub-groups is a potential solution to answer these questions and to tackle the single atlas problem, and several methods have been proposed accordingly. Blezek and Miller [1] developed an atlas stratification method to infer multiple MR brain atlases in a population of subjects in contrast to the traditional methods that assume a single atlas for the whole population, and to infer which subjects should be used to construct the atlas for each sub-population, by adopting the mean shift method [3] to perform clustering in the population. However, this method is quite computational expensive. Sabuncu et al. [4] recently proposed a method for discovering patterns from a MR brain image population through mixture modeling. In this method, the number of cluster in the population has to be manually defined before clustering.

In this paper, we proposed a novel method for grouping 3D human brain MR images into different clusters. We use affinity propagation [5] to perform clustering on a population of

brain MR images. After clustering, in each cluster (called a sub-population), a representative exemplar image is identified as the single subject atlas for the sub-group. Meanwhile, all the subject images belonging to the same sub-group are identified. The number of clusters is automatically determined in the affinity propagation. The method has been applied on a dataset including 414 subject brain MRI images. Our preliminary experiment results demonstrate the effectiveness of the proposed method.

II. METHODS

A. Similarity between brain MR images

Before performing brain MR image clustering, we firstly define the similarity between a pair of images. Previously, people employed mean square error or mutual information based on intensity values to measure the similarity between brain MR images [1,4]. However, a potential problem is that the intensities in brain MR images might be affected by the inhomogenous bias field and noise. Therefore, the mean square error and mutual information measurements might not be quite robust for the comparison of a pair of brain MR image. Actually, the human brain MR image is mainly composed of three distinct types of tissues: white matter (WM), grey matter (GM) and cerebrospinal fluid (CSF). Each tissue can be further parcellated into different neuroanatomic meaningful structures. Therefore, instead of using intensity values in MR images directly, we adopt the tissue-segmented and anatomically-parcellated images for comparing a pair of brain MR images.

B. Similarity based on tissue-segmented images

The tissue segmentation is accomplished via FAST [6] in the FSL software package, which uses the hidden Markov random field and expectation maximization method for tissue segmentation and has been proved to be the-state-of-the-art method. Figure 1 (b) shows an example of the tissue segmentation result on a brain MR image. Before segmentation, the subject images have been skull-stripped and spatially normalized to the same space using affine transform. Therefore, the similarity between two tissue-segmented brain MR images is defined as:

$$s(A,B)=\frac{V(A_{WM}\cap B_{WM})+V(A_{GM}\cap B_{GM})+V(A_{CSF}\cap B_{CSF})}{V(A\cup B)} \quad (1)$$

where A and B represent two brain MR images, and A_{WM} and B_{WM} represent the white matter regions in image A and B, respectively. Similarly, the subscript *GM* and *CSF* represent gray matter and cerebrospinal fluid regions, respectively. $V(.)$ is the volume of the region. The operator ∩ and ∪ take the intersection and union of two regions, respectively. This definition implies that similar tissue structures produce high similarity.

C. Similarity based on parcellated images

To compare the brain MR images in a more detailed anatomical level, the images are further parcellated into fine-detailed neuroanatomic regions using the high-dimensional hybrid registration method [7,8]. Figure 1 (c) shows an example of brain structure segmentation result on a brain MR image. The similarity between two parcellated brain MR images is defined as:

$$s(A,B)=\frac{\sum_i V(A_i\cap B_i)}{V(A\cup B)} \quad (2)$$

where A and B represent two brain MR images, and A_i and B_i represent the i^{th} parcellated regions in image A and B, respectively. $V(.)$ is the volume of the region. The operator ⋂ and ⋃ take the intersection and union of two regions, respectively. This definition implies that similar anatomic structures produce high similarity.

D. Image clustering via affinity propagation

Once the similarity between each pair of subject images is obtained, we adopt the affinity propagation (AP) clustering method [5] to perform the brain MR image grouping. The affinity propagation method is a recently proposed clustering method that can automatically determine the number of clusters in the population. The affinity propagation method has been proved to have better performance than traditional k-means clustering method [5]. In general, affinity propagation works by finding a set of exemplars in the data and assigning other data points to the exemplars. The affinity propagation algorithm approximates maximization of the sum of similarities to exemplars by recursively passing real-valued message along edge in a factor graph until a good set of exemplars and corresponding clusters emerges. Basically, there are two kind of messages exchanged between data points, responsibility and availability, and each takes a different type of competition into account. The inputs are the pair-wise similarities and data point preferences.

In affinity propagation, the similarity $s(i,k)$ indicates how well the data point k is suited to be the exemplar for data point i. The preference $s(i,i)$ is defined such that points with high values are more likely to be chosen as exemplars. The number of identified exemplars is influenced by both the values of the input preference and the messaging-passing procedure. The responsibility $r(i,k)$, sent from data point i to a candidate exemplar point k, reflects the accumulated evidence for how well-suited point k is to serve as the exemplar for point i, taking into account other potential exemplars for point i. The self-responsibility $r(k,k)$ reflects accumulated evidence that point k is an exemplar based on its input preference tempered by how ill-suited it is to be assigned to another exemplar. The availability $a(i,k)$, sent from candidate exemplar point k to point i, reflects the accumulated evidence for how appropriate it would be for point i to choose point k as its exemplar, taking into account the support from other point that point k should be an exemplar. The availability $a(k,k)$, reflects accumulated evidence that point k is an exemplar, based on the positive responsibilities sent to candidate exemplar k from other points. The affinity propagation is performed as follows:

Initially, the availabilities are set to be zero: $a(i,k) = 0$. The responsibilities are computed as:

$$r(i,k) \leftarrow s(i,k) - \max_{k' \neq k}\{a(i,k') + s(i,k')\}$$

The availabilities are updated as:

$$a(i,k) \leftarrow \min\{0, r(k,k) + \sum_{i' \notin \{i,k\}} \max\{0, r(i',k)\}\}$$

The self-availability $a(k,k)$ is updated differently as:

$$a(k,k) \leftarrow \sum_{i' \neq k} \max\{0, r(i',k)\}\}$$

The responsibility update lets all of the candidate exemplars compete for ownership of a data point, whereas the availability update collects evidence from data point as to whether

each candidate exemplar would be a good exemplar. The messages of availability and responsibility are updated recursively. After convergence, availabilities and responsibilities are combined to identify exemplars. For point i, the value of k that maximizes $a(i,k) + r(i,k)$ either identifies point i as an exemplars if $k = i$, or identify data point that is the exemplar for point i. More details of the affinity propagation method could be found in [5].

III. RESULTS

In this section, a set of experiments are conducted to evaluate the proposed method. We adopt the two similarity measures for affinity propagation in Section II to perform grouping. In all experiments, we use the publicly available OASIS neuroimaging dataset [9], which contains 414 preprocessed human brain MR images of subjects with the age range from 18 to 91 years.

A. Experiment 1

In this experiment, we adopt the similarity between tissue-segmented brain MR images for clustering (Section II). In affinity propagation, the preferences are set to be 0.3 times the minimum of the similarity matrix for all images, since we do not know which images are more likely to be chosen as exemplars and the small preferences tend to produce small number of clusters. After clustering, we identified 4 distinct clusters which contain 147, 112, 73 and 82 subject images, respectively. The exemplars of each cluster are shown in Figure 2. In Figure 2, (a), (b), (c) and (d) represent the exemplars of the four identified clusters respectively. As we can see, one obvious difference in the 4 exemplars is in the lateral ventricle. Figure 2(a) and (b) (cluster 1 and 2) have relative small lateral ventricle, and Figure 2(c) (cluster 3) has middle size lateral ventricle, and Figure 2(d) (cluster 4) has large size lateral ventricle. To further demonstrate the difference of the 4 clusters, we average the images in each cluster to create the average image for each cluster. Figure 2(e), (f), (g) and (h) represent the average images, corresponding to cluster 1, 2, 3 and 4, respectively. The differences of lateral ventricles are also observed in the averaged images among the four clusters.

We also analyze the age distributions in the 4 identified cluster as shown in Figure 3. The density of age distribution is estimated by the kernel smoothing method with a Gaussian kernel and the bandwidth of 4 years. As we can see, cluster 1 and 2 mainly consist of young and middle aged subjects, while cluster 3 and 4 mainly consist of old aged subjects. From Figure 3, we can see that the old aged subjects tend to have relative large lateral ventricle, though some individual old aged subjects might have small ventricles. The young and middle aged subjects tend to have small lateral ventricles. Therefore, we could conclude that the dominant structure patterns in the population are mainly due to aging. This result is very similar to the finding in [4].

B. Experiment 2

In this experiment, we adopt the similarity between parcellated brain MR images for clustering (Section II). In affinity propagation, the preference is set as the same method as that in experiment 1. After clustering using affinity propagation, again, we find 4 distinct clusters which contain 80, 138, 144 and 52 subject images, respectively. The exemplars of each cluster are shown in Figure 4. In Figure 4, (a), (b), (c) and (d) represent the exemplars of the 4 identified cluster 1, 2, 3 and 4, respectively. As we see, one obvious difference among the four exemplars is in the lateral ventricle. Figure 4(a) and 4(b) (cluster 1 and 2) have relatively small lateral ventricle, and Figure 4(c) (cluster 3) has middle size lateral ventricle, and Figure 4(d) (cluster 4) has large size lateral ventricle. To further demonstrate the difference of the four clusters, we average the images in each cluster to create the

average image for each cluster. Figure 4(e), (f), (g) and (h) represent the average images corresponding to cluster 1, 2, 3 and 4, respectively. The differences of lateral ventricle are also observed in the averaging images in the 4 clusters. The density of age distribution, which is estimated by the kernel smoothing method with a Gaussian kernel and the bandwidth of 4 years, is shown in Figure 5. Similarly, as we can see, cluster 1 and 2 mainly consist of young and middle aged subjects, while cluster 3 and 4 mainly consist of old aged subjects. This result is similar to the result in experiment 1 and the finding in [4]. These results in experiment 1 and 2 demonstrate that the method can effectively identify the patterns in a population of brain MR images.

IV. DISCUSSION AND CONCLUSION

In this paper, we proposed a novel method for grouping brain MR images into different patterns. The method adopts affinity propagation to perform clustering and uses the tissues-segmented and parcellated image to compare brain MRI images. The major advantages of this method over previous ones, e.g., those in [1,4], are its efficiency and automation. The method has been applied to the OASIS neuroimaging dataset and promising results have been obtained. The method itself is general and it is applicable to other kinds of similarities in brain MR image. The future work includes: 1) use the identified exemplars in each cluster as a single atlas to carry out atlas based brain image analysis in each cluster, e.g., brain image registration; 2) group specific anatomical structure in brain MR images and studying the variability of human brain with this method; and 3) perform quantitative comparisons with other methods such as those in [1,4].

Acknowledgments

The authors would like to thank Dr. Randy Buckner for making the OASIS dataset publicly available. Dr. T Liu was partly supported by the NIH/NIBIB Career Award EB 006878 and The University of Georgia start-up funding.

REFERENCES

1. Blezek D, Miller J. Atlas stratification. Medical Image Analysis 2007 Oct;vol. 11:443–457. [PubMed: 17765003]
2. Joshi S, Davis B, Jomier M, Gerig G. Unbiased diffeomorphism atlas construction for computational anatomy. NeuroImage 2004;vol. 23:S151–S160. [PubMed: 15501084]
3. Comaniciu D, Meer P. Mean shift: a robust approach toward featue space analysis. IEEE Trans. Pattern Analysis and Machine Intelligence 2002 May;vol. 24:603–619.
4. Sabuncu MR, Balci SK, Golland P. Discovering modes of an image population through mixture modeling. MICCAI 2008. LNCS 2008;vol. 5242:381–389.
5. Frey BJ, Dueck D. Clustering by passing message between data points. Science 2007;vol. 315:972–976. [PubMed: 17218491]
6. Zhang Y, Brady M, Smith S. Segmentation of brain MR images through a hidden Markov random field model and expectation-maximization algorithm. IEEE Trans. on Medical Imaging 2001 Jan;vol. 20:45–57.
7. Liu T, Shen D, Davatzikos C. Deformable registration of cortical structures via hybrid volumetric and surface warping. NeuroImage 2004 Aug;vol. 22:1790–1801. [PubMed: 15275935]
8. Shen D, Davatzikos C. HAMMER: hierarchical attribute matching mechanism for elasctic registration. IEEE Trans. On Medical Imaging 2002 Nov;vol. 21:1421–1439.
9. Marcus DS, et al. Open Access Series of Imaging Studies (OASIS): cross-sectional MRI data in young, middle aged, nondemented, and demented older adults. Journal of Cognitive neuroscience 2007;vol. 19:1498–1507. [PubMed: 17714011]

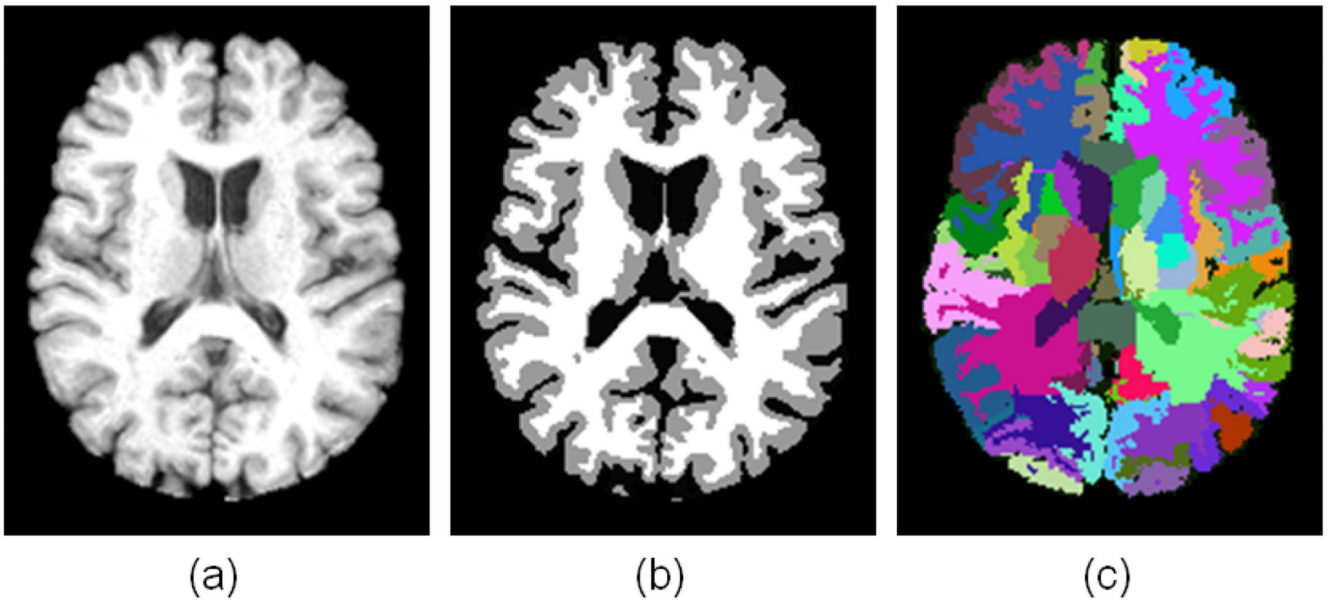

Figure 1.
An example of tissue segmentation and structure parcellation results on a brain MR image. (a) is the original image. (b) is the corresponding tissue segmentation result. (c) is the corresponding structure parcellation result.

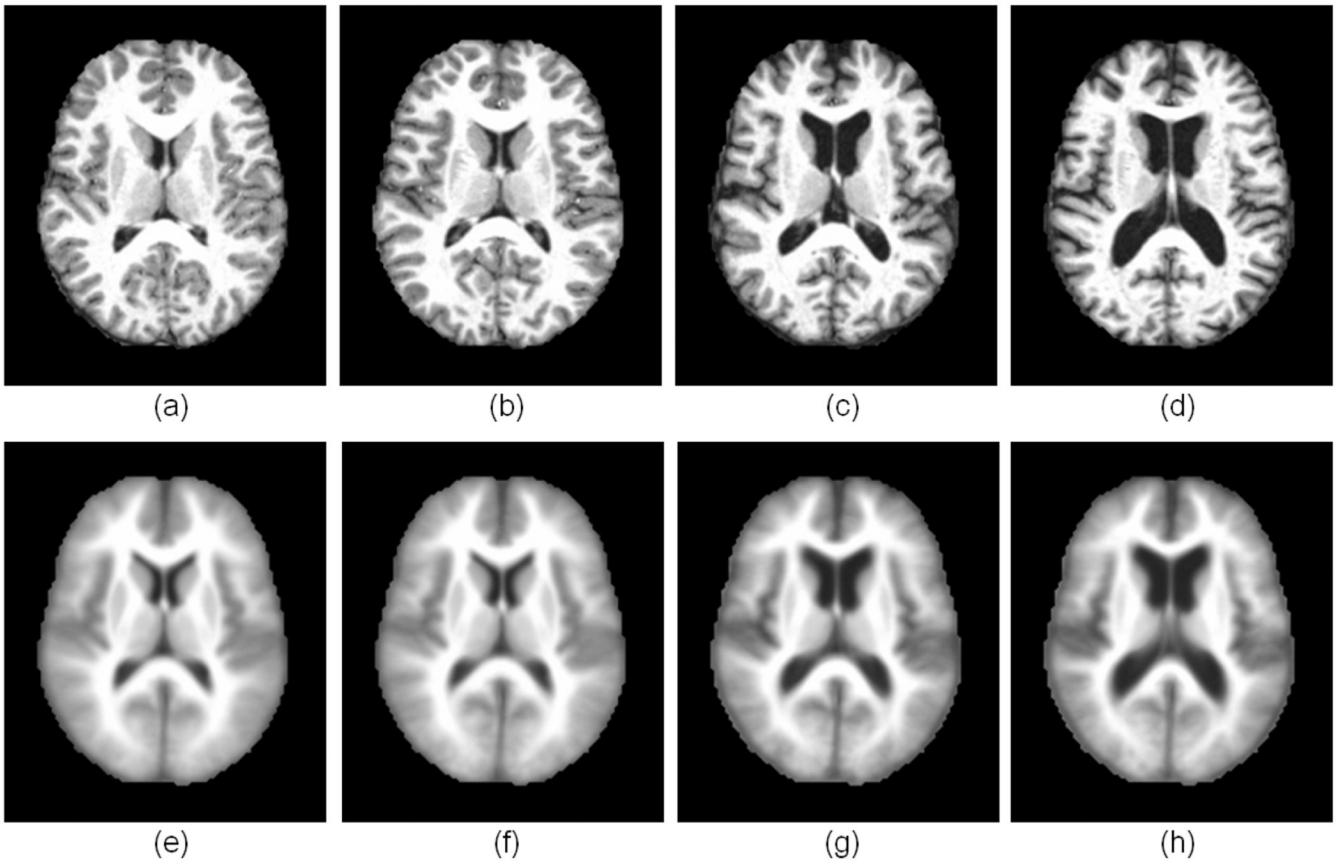

Figure 2.
The brain MR image clustering results in experiment 1. The top row shows the exemplars in the 4 identified clusters. The bottom row shows the corresponding average images in the 4 clusters. As we see, the method is able to find the 4 distinct clusters in the population. One obvious difference in the 4 clusters is in the lateral ventricle.

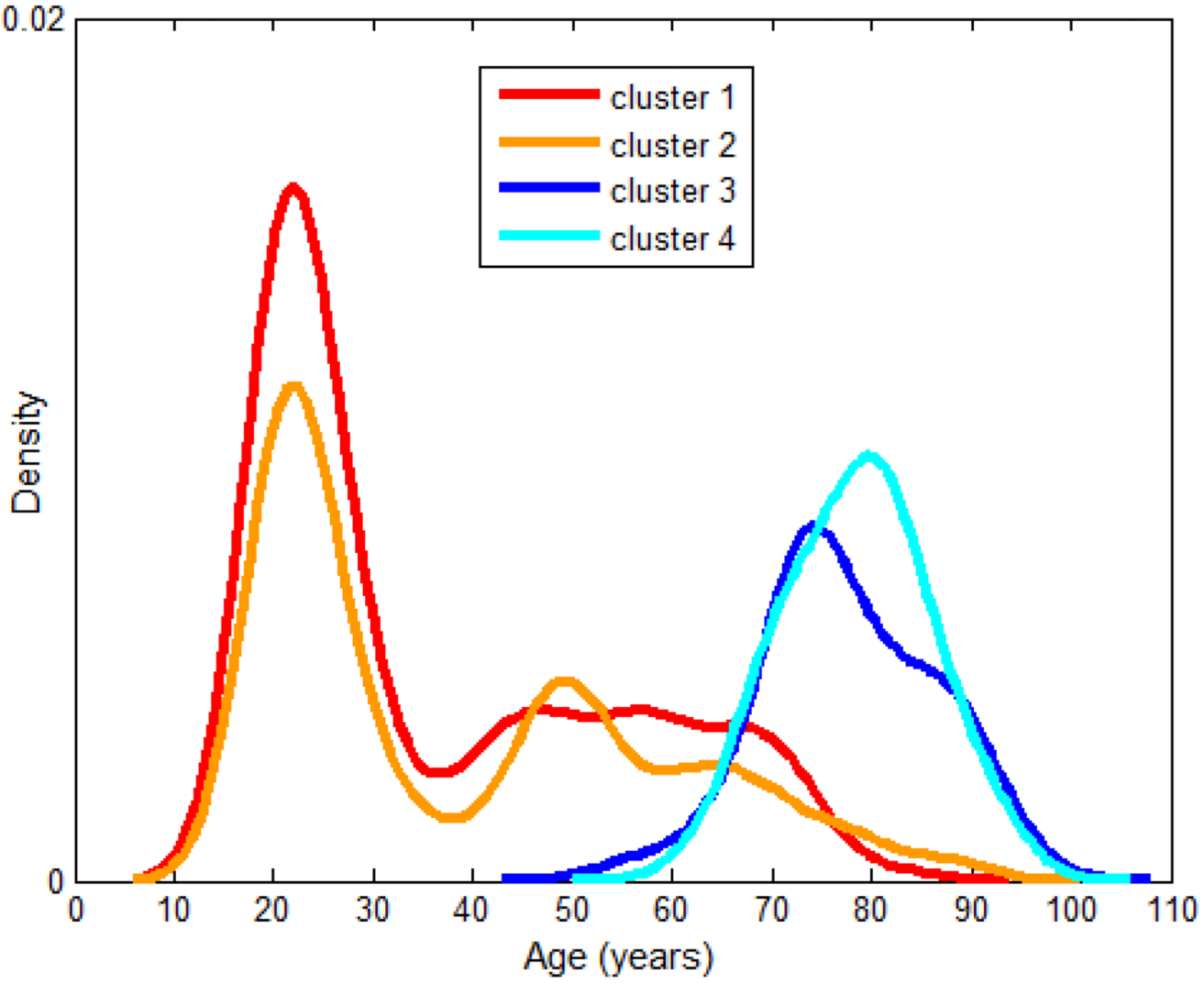

Figure 3.
The age distribution of 4 identified cluster in experiment 1. As we can see, cluster 1 and 2 are mainly composed by young and middle aged subjects, whereas cluster 3 and 4 are mainly composed by old aged subjects.

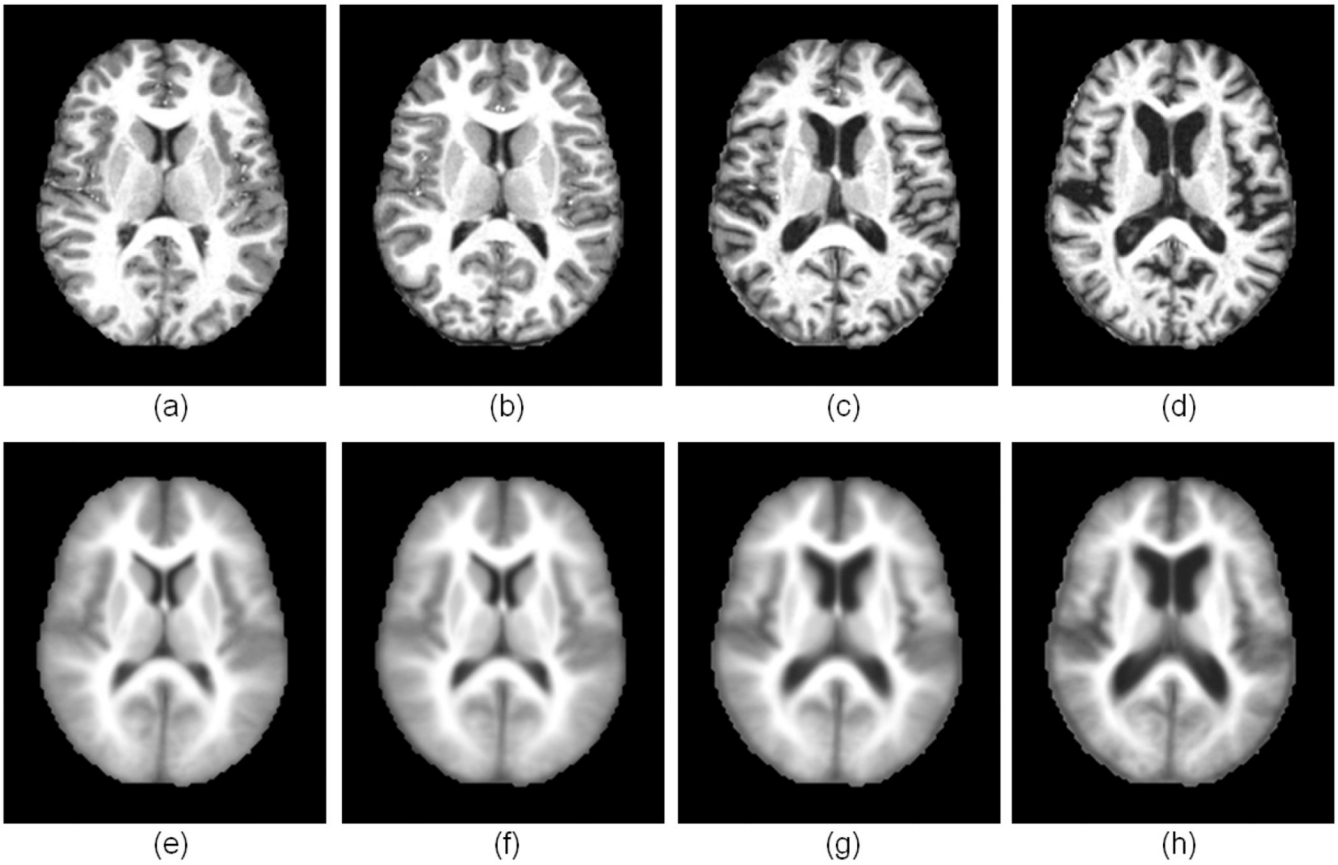

Figure 4.
The brain MR image clustering results in experiment 2. The top row shows the exemplars in the 4 identified clusters. The bottom row shows the corresponding averaging images in the 4 cluster. As we see, the method is able to find the 4 distinct clusters in the population. One obvious difference in the 4 clusters is the lateral ventricle.

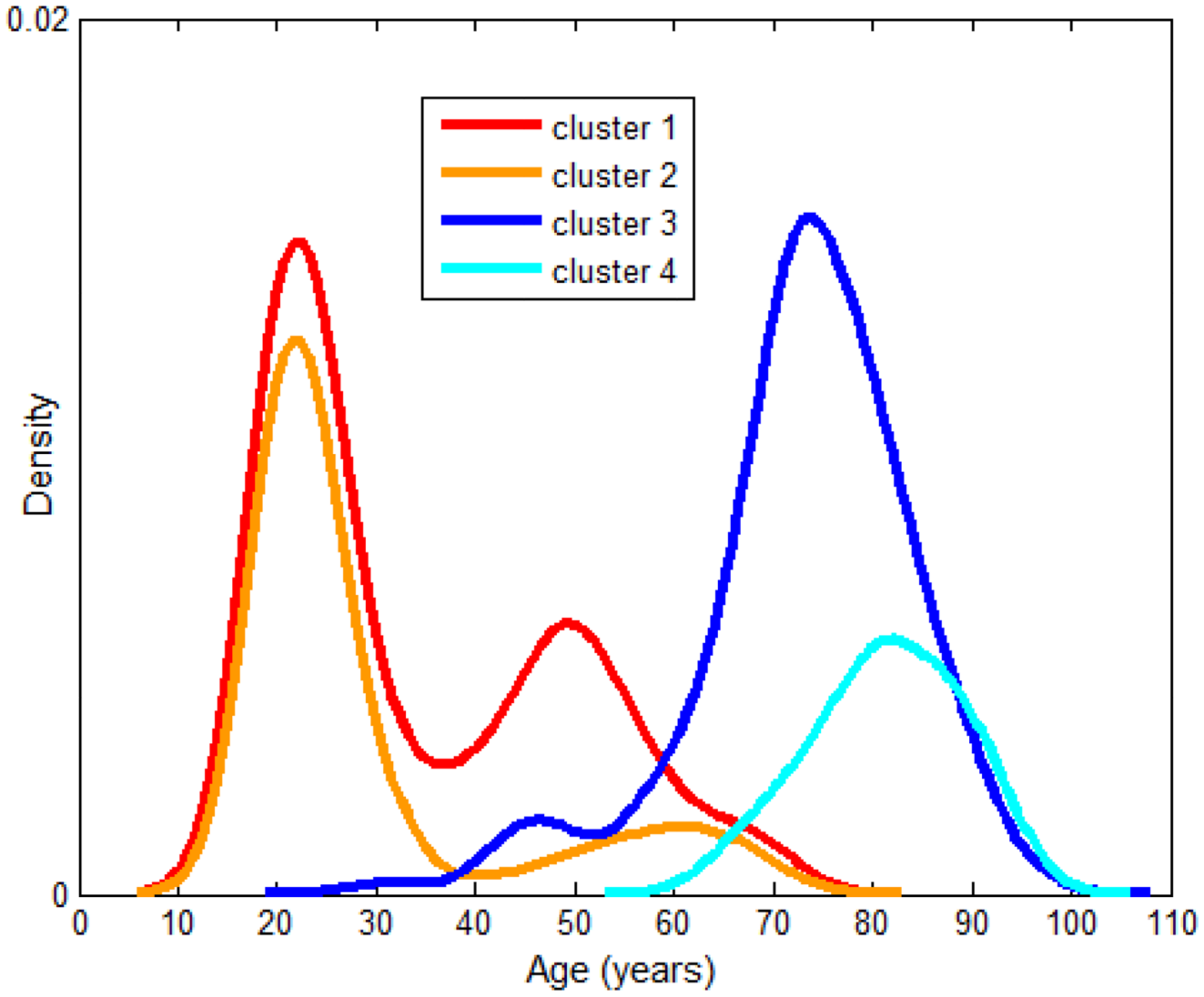

Figure 5.
The age distribution of 4 identified cluster in experiment 2. As we can see, cluster 1 and 2 are mainly composed by young and middle aged subjects, whereas cluster 3 and 4 are mainly composed by old aged subjects.